The triple GEM detector as beam monitor for relativistic hadron beams

2014 JINST 9 P06006

(http://iopscience.iop.org/1748-0221/9/06/P06006)

PUBLISHED BY IOP PUBLISHING FOR SISSA MEDIALAB

RECEIVED: *February 27, 2014*
ACCEPTED: *April 21, 2014*
PUBLISHED: *June 5, 2014*

The triple GEM detector as beam monitor for relativistic hadron beams

E. Aza,[a,b,1] **M. Magistris,**[a] **F. Murtas,**[a,c] **S. Puddu**[a,d] **and M. Silari**[a]

[a] *CERN,*
Geneva 23, 1211 Geneva, Switzerland
[b] *Department of Physics, AUTH,*
54124 Thessaloniki, Greece
[c] *LNF-INFN,*
Via Fermi 40, 00044, Frascati, Italy
[d] *AEC-LHEP, Bern University,*
Sidlerstrasse 5, 3012 Bern, Switzerland

E-mail: eleni.aza@cern.ch

ABSTRACT: A triple GEM detector was tested at the CERF facility at CERN as an on-line beam imaging monitor and as a counting reference device. It was exposed to a 120 GeV/c positively charged hadron beam (approximately 2/3 pions and 1/3 protons), which hits a copper target generating a wide spectrum of different kinds of particles used for various experiments. The flux of beam particles ranged over three orders of magnitude, from $8 \cdot 10^4$ s^{-1} to $8 \cdot 10^7$ s^{-1}. The profile of the beam acquired with the GEM was compared to the one measured with a MWPC and no saturation was observed. In addition, the count rate measured with the GEM was compared to the one measured with an Ionization Chamber, which is routinely used for monitoring the beam intensity. Another way of monitoring the intensity of the beam was also explored, which is based on the total current driven from the GEM foils. The digital readout allows making a 2D online image of the beam for the alignment with the copper target in the CERF facility. A low residual activation of the detector was observed shortly after irradiation.

KEYWORDS: Micropattern gaseous detectors (MSGC, GEM, THGEM, RETHGEM, MHSP, MICROPIC, MICROMEGAS, InGrid, etc); Beam-line instrumentation (beam position and profile monitors; beam-intensity monitors; bunch length monitors)

[1] Corresponding author.

doi:10.1088/1748-0221/9/06/P06006

Contents

2014 JINST 9 P06006

1 Introduction

A triple GEM (Gas Electron Multiplier) detector [1] was used as a beam monitor at the CERN-EU high-energy Reference Field (CERF) [2] facility at CERN. CERF is installed in one of the secondary beam lines (H6) from the Super Proton Synchrotron (SPS) at CERN. A 120 GeV/c positively charged hadron beam composed of 61% π+, 35% p+ and 4% K+ hits a cylindrical copper target generating a wide spectrum of different kinds of particles which can be detected in various positions inside the irradiation cave and on the top of the iron and concrete roof-shielding. The beam extraction time (spill) from the SPS lasts 9.5 s over a 45 s cycle. The beam intensity is approximately constant, producing a constant irradiation field at the exposure locations. The intensity can be adjusted by two collimators in the beam line, which control the horizontal and vertical acceptance.

The neutron spectrum produced on the concrete roof resembles the field created by cosmic rays at commercial flight altitudes, so that instrumentation can be tested, inter-compared and calibrated in this reference field in order to be used for in-flight measurements on aircraft. A layout of the experimental area is shown in figure 1. The target can be installed in two different positions inside the irradiation cave.

The profile of the beam is normally measured with a Multi-Wire Proportional Chamber (MWPC) installed in-between the two target positions. The intensity of the primary beam is monitored by an air-filled ionisation chamber (IC) [3, 4] at atmospheric pressure, placed in the beam just upstream of the copper target. A triple GEM detector with a 1 μm aluminium cathode was used as a beam monitor between the MWPC and the copper target. The GEM was mounted on a stand aligned to the centre of an aluminium tube that replaced the target for these measurements

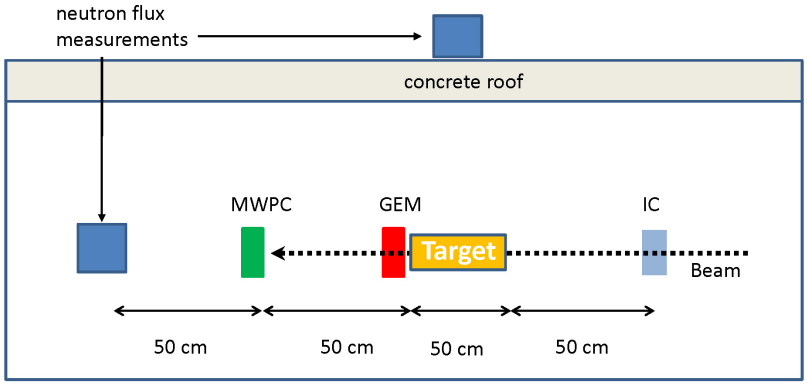

Figure 1. CERF facility layout.

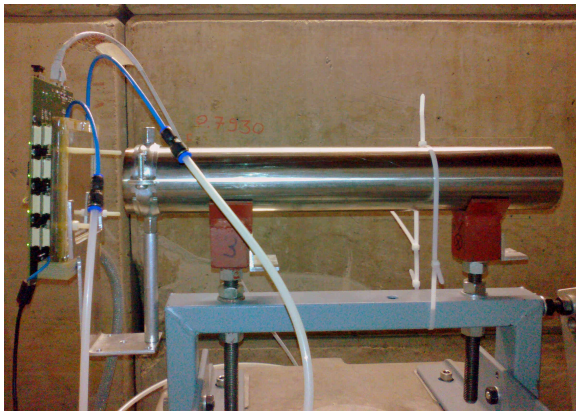

Figure 2. Experimental set-up. The GEM detector on the left is aligned to the aluminium tube (target position). The beam is impinging from right to left.

(figure 2). The beam intensity is adjusted by two collimators in the beam line, which control the horizontal and vertical acceptance.

Up to now the beam set-up on the target was done using Polaroid films, which are no longer in production and more and more difficult to find on the market, and in addition require a lengthy procedure. The Triple GEM detector appears to be an interesting alternative. The detector has been previously tested [5, 6] as a beam monitor for high energy hadron beams, but at lower beam intensity and smaller active area. This is the first time it has been used to provide a 2D online beam image and at the same time measure the beam intensity via the current driven by the foils.

2 The triple GEM detector

The triple GEM detector consists of three 50 μm thick insulating kapton foils [7], clad on each side with a thin copper layer of 5 μm and chemically perforated with a high density of holes with a bi-conical structure of 70 μm external and 50 μm internal diameter and a pitch of 140 μm. The device is equipped with a thin aluminium cathode, has an area of $5\times5\,\mathrm{cm}^2$ and it is filled with Ar/CO_2 (70/30) gas. The GEM foils are sandwiched between two parallel electrodes; the upper electrode plays the role of the cathode and the lower one of the anode (figure 3). If a suitable voltage is

2014 JINST 9 P06006

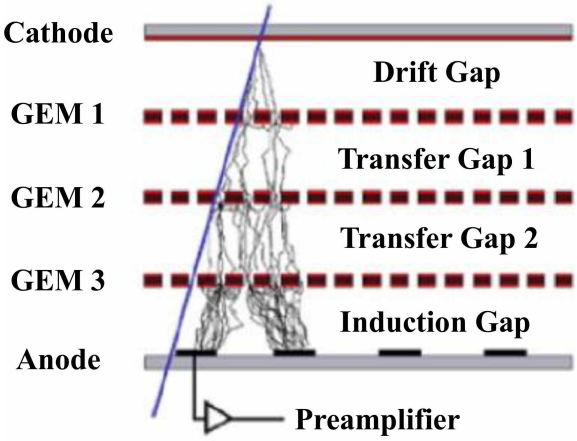

Figure 3. The triple GEM detector.

applied to the foils, a strong electric field is generated in the holes so that electrons can acquire enough energy to develop an avalanche with a gain of more than 10^3.

In a triple GEM it is possible to recognize the following regions:

- Drift region: here the detected particles ionize the gas, due to the drift field, ions move to the cathode and electrons to the first GEM foil. The 3 mm gap is small enough to avoid space charge effects.
- Two Transfer regions of 1 mm and 2 mm, respectively, where the field guides the electrons to the following GEM foils in order to achieve a higher gain. The first Transfer region should be as narrow as possible in order to minimize the primary ionization from background particles producing a detectable signal. On the other hand, a wider second Transfer region reduces the discharge probability in the induction region [8].
- Induction region: here the electron cloud induces the signal on the pad. The region thickness is 1 mm.

The detector gain depends on the high voltages V_i applied to the GEM foils so that $G \propto e^{\Sigma Vi}$. The working point chosen was 900 V that corresponds to gain 300. The reason for choosing a low gain is because of the relatively high particle flux, in order to lower the efficiency of the detector and avoid discharge and saturation effects. In principle a double GEM could also be employed, but discharge phenomena are fewer if the same gain is shared between three foils rather than two.

The signal generated by the electron cascade is induced on a padded anode. The anode consists of a total of 128 pads with 6×3 mm^2 area each, organized in an 8×16 matrix. The read-out is kept at ground potential and is connected to the front-end electronics. The signals from the pads are pre-amplified, shaped and discriminated by eight CARIOCA-GEM digital chips [9]. All the CARIOCA chips are connected to a custom made FPGA Mother Board [10] attached to the back of the detector that analyses the LVDS signal coming from the chips. The FPGA board is able to perform count and time measurements of discriminated signals coming from the 128 channels and can collect multiple gates into memory with negligible dead time, allowing an external or an internal trigger. The high voltage system used to power the GEM foils is the HVGEM NIM module [11]. It consists of seven

2014 JINST 9 P06006

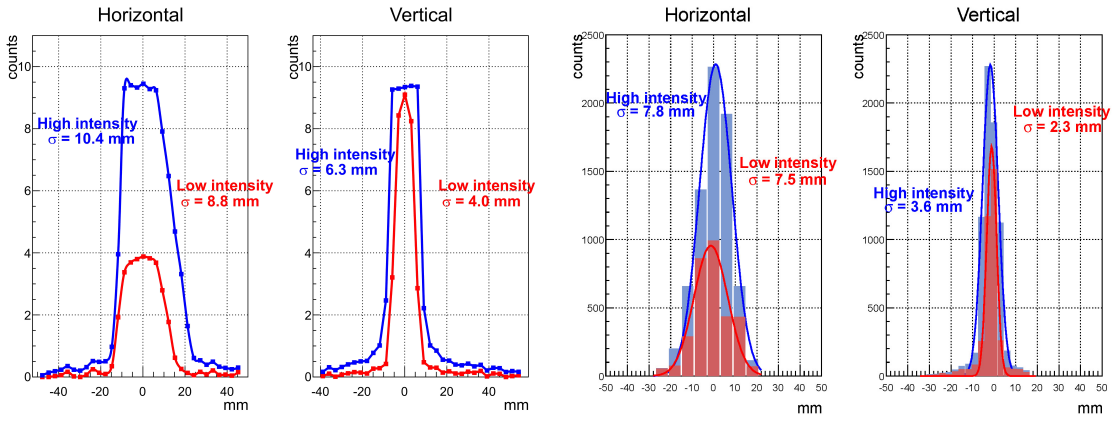

Figure 4. a) Beam profile from the MWPC. The chamber saturates at high intensity. b) Beam profile from the GEM, well-fitted with a Gaussian curve.

independent HV channels referred to ground, six of which can provide up to 700 V and one up to 1400 V, allowing higher portability of the GEM detector, as well as flexibility in the application of the desired voltage to each foil. In addition, each channel is equipped with a high sensitivity current meter for the detection of possible discharges and the current driven by the detector with 10 nA precision.

3 Measurements of beam profile and intensity

The beam profile was measured with both the MWPC and the GEM and compared for different intensities. In addition, the linearity of the two detectors was investigated with the total current driven by the GEM foils and with digital readout.

3.1 GEM versus Multi Wire Proportional Chamber

Multi Wire Proportional Chambers (MWPC) are used in many transfer lines and experimental areas at CERN. They can provide reliable X and Y profile measurements but present some limitations, such as saturation at high intensities and limited spatial resolution. In order to try and overcome these constraints, the beam profile obtained with the MWPC and the GEM was compared.

The vertical and horizontal position of the beam and the sigma of the associated Gaussian distributions were determined with the MWPC (figure 4a) and the GEM (figure 4b). The beam line collimators were adjusted in order to obtain the desired beam intensity. The flux of beam particles ranged from $8 \cdot 10^4\ s^{-1}$ to $8 \cdot 10^7\ s^{-1}$ and a scan was performed in this intensity range. By progressively opening the collimators we observed that the beam remained aligned on the target with increasing intensity, but with a slight diffusion. Figure 4a shows that at high intensity the MWPC saturated, which increases the uncertainty of the sigma of the Gaussian distribution. In particular, the horizontal collimator had a higher impact on the beam spot size.

The mean and the sigma of the beam as measured with the GEM detector are plotted in figure 5a and figure 5b, respectively. The position of the beam in both directions remained the same

2014 JINST 9 P06006

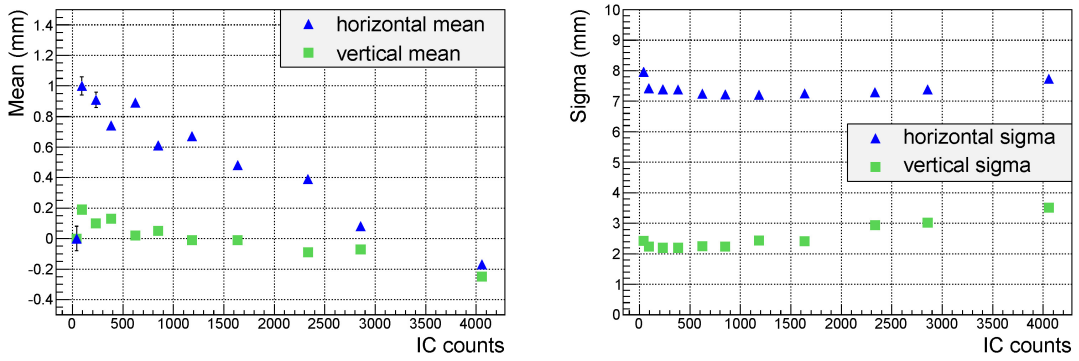

(a) **(b)**

Figure 5. a) Mean of the beam profile. The shift of the horizontal mean is within the beam dimensions. b) Sigma of the beam profile. The sigma increases with increasing intensity in the vertical direction.

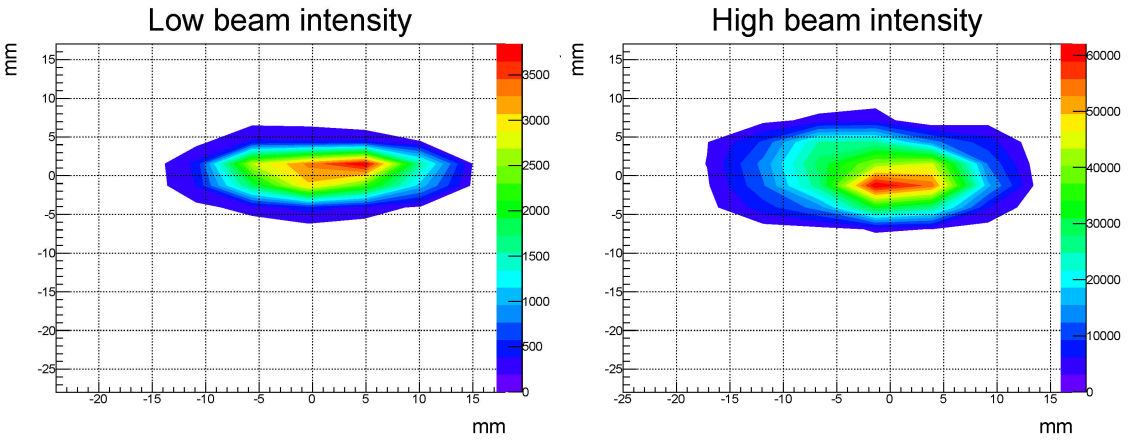

(a) **(b)**

Figure 6. a) Beam profile at low intensity with $\sigma_x = 7.6$ mm and $\sigma_y = 2.4$ mm. Mean at point (0,0). b) Beam profile at high intensity with $\sigma_x = 8.0$ mm and $\sigma_y = 3.5$ mm. Mean shifted to point (-0.2, -0.3).

with negligible fluctuations, while the sigma increased when increasing beam intensity. It should be noted that the beam dimensions did not increase symmetrically, as shown in figure 6a and figure 6b.

3.2 GEM total current versus Ionization Chamber counts

The beam impinging on the target was spilled from the SPS and the particle flux was not exactly constant during the spill. This flux could be measured both via the IC counts [3, 4] and via the total current driven by the GEM foils, read by the HVGEM module during the spill. A typical time distribution in step of one second during one spill as recorded from the IC in high beam intensity is shown in figure 7. Due to asynchronization between the GEM and the IC gates, the first and the last acquisition of the spill were not taken into account. As displayed in figure 7 there is reasonable correspondence between IC counts and current.

The correlation is illustrated in figure 8 with data taken for five spills with two different high beam intensities, fitted with a linear function, which results in 0.26 ± 0.03 nA per IC count. Taking

2014 JINST 9 P06006

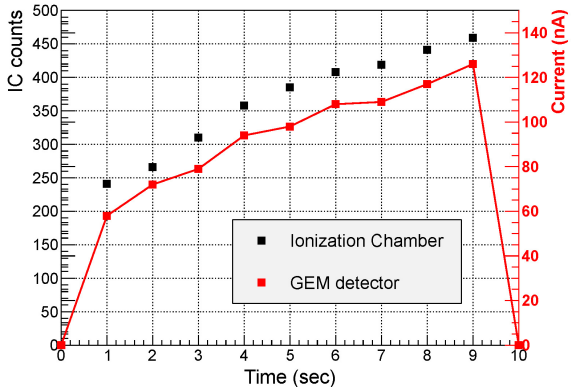

Figure 7. Particle flux measured by the IC and total GEM current from one spill.

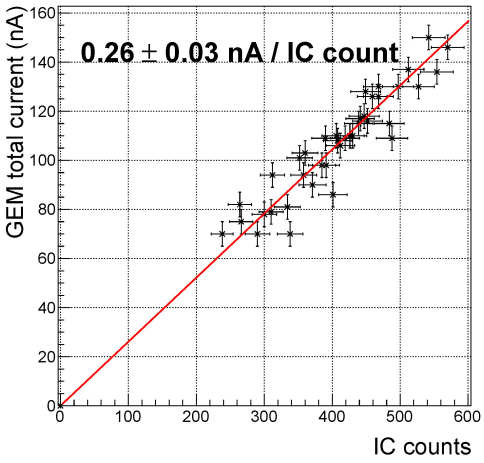

Figure 8. Correlation between IC counts and GEM current. The calibration value is displayed on top of the figure.

the IC calibration factor of $2.2 \pm 0.2 \cdot 10^4$ particles per count into account, we obtain $8.5 \pm 1.4 \cdot 10^4$ beam particles per nA, which can be used for monitoring the intensity of the beam. In the future this procedure can be accomplished on line by implementing the calculation of the total current each second inside the HV acquisition program.

3.3 GEM versus Ionization Chamber counts

Good correlation was found between GEM and IC counts during the intensity scan. For each intensity the data were acquired from three spills; the statistical error of the mean values is displayed in figure 9.

A systematic error in the number of counts from the GEM was found for beam intensities higher than $4 \cdot 10^6\,\mathrm{s}^{-1}$ corresponding to 1800 IC counts per spill. These errors arise from:

1. The dead time of the detector: 20%.

2. The random statistical error in the counting rate of the detector: 0.1%.

2014 JINST 9 P06006

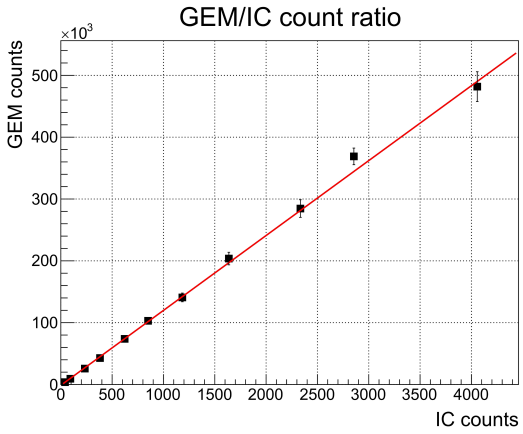

Figure 9. GEM/IC count ratio fitted with the first six points.

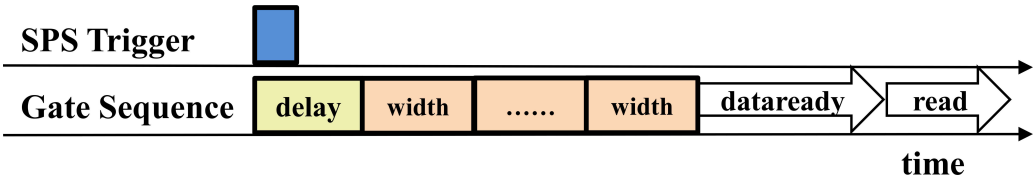

Figure 10. FPGA acquisition mode. The gate sequence of width 0.5–1 s can be processed and stored after a desired delay (0–2.7 s). An external trigger from the SPS can be applied. Data can be read and stored after a defined number of gates.

3. A percentage of lost counts on the GEM due to sparks and masked noisy channels: 1–2%.

4. A percentage from lost counts due to the limited dimensions of the active area of the detector with respect to the beam size: 1–1.5%.

The dead time is the ratio of the time during which the detector is inactive to the total acquisition period. The dead time is due to limitations of the acquisition system because online measurements and plots need to be refreshed for each event. For future measurements, this dead time can be reduced to a negligible level by using an FPGA mode which reads and stores data after a maximum of 255 gates instead after each event (figure 10). In addition, the trigger of the SPS will be used for the gate sequence.

We observed interruptions in the functioning of the FPGA at high beam intensities, probably because the FPGA was mounted on the back side of the detector and thus the electronics was directly exposed to the beam.

Regarding the lost counts due to sparks and noise, two channels at the centre of the beam distribution were masked and two channels at the edge of the active area were found to be very sensitive to rare discharges. In both cases the per cent error was calculated from the mean of the counts coming from the eight pads surrounding each discarded channel.

In addition, at high intensity the dimension of the beam in the horizontal direction slightly exceeded the detector's active area. Therefore a minor fraction of the primary particles missed the detector.

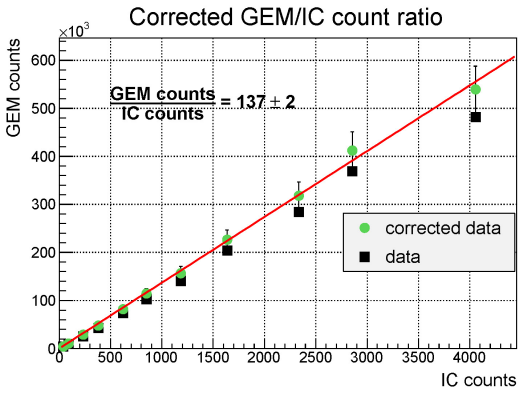

Figure 11. GEM/IC corrected count ratio.

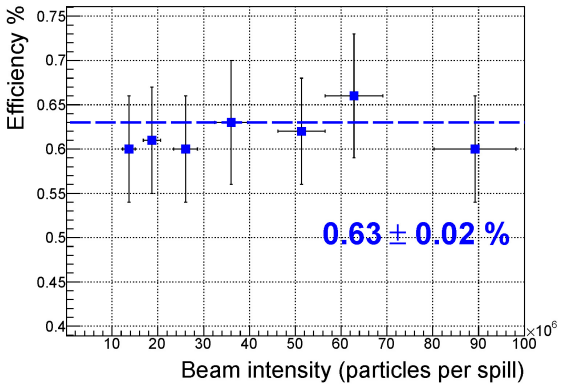

Figure 12. Per cent detector efficiency as a function of the beam intensity per spill.

The mentioned systematic errors resulted in a large positive error of 22.6% and a small 2.6% negative error. After the data were corrected for these errors, the correlation between GEM and IC counts appears more linear as shown in figure 11.

Finally, a calibration factor of 137 ± 2 particles per count was found for the GEM detector.

4 GEM detector efficiency

The efficiency was measured as the ratio of the detected number of hits to the impinging particles for different intensities, determined by means of the calibration factor of $2.2 \pm 0.2 \cdot 10^4$ particles per IC count [3, 4]. The efficiency appeared to be rather constant in the range from 10^7 to 10^8 particles per spill (figure 12), with a mean value of $0.63 \pm 0.02\%$.

The low gain (300) chosen for the measurements resulted in low efficiency, since the beam is composed of minimum ionizing particles. High gain was avoided because of possible saturation and discharge effects, thus ensuring more reliable results.

2014 JINST 9 P06006

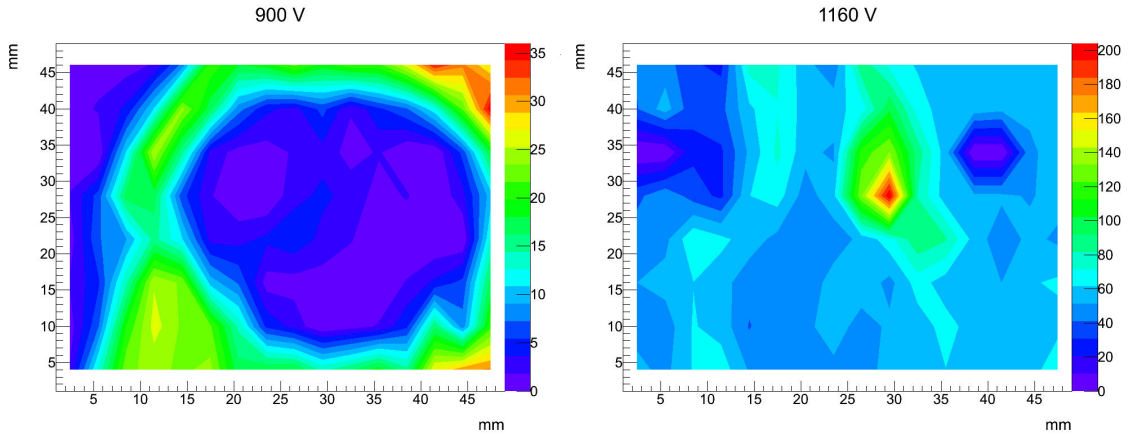

(a) **(b)**

Figure 13. a) Signal due to residual activation of the GEM. Applied voltage 900 V. b) Signal due to residual activation of the GEM. Applied voltage 1160 V.

5 Detector activation

Sensitivity and stability studies have shown that the GEM detector's components can be activated when irradiated with a high flux of energetic particles [12]. In order to investigate this phenomenon, the detector was switched on seven hours after the intensity scan described in section 3.1. The distribution observed on the active area is displayed in figure 13a with an applied voltage of 900 V. Increasing the voltage to 1160 V, the distribution transformed to the one in figure 13b.

The activation of the detector is probably responsible for the signal acquired with the beam off. The distribution in figure 13a can be produced by high ionizing particles, such as alpha particles, or x-rays because it was observed at low gain. The material composition of the device is mostly copper, which can be activated by high energy hadrons. This phenomenon is still under investigation via the FLUKA simulation code [13, 14].

With the beam off the total number of counts per second in figure 13b was $144\,s^{-1}$, while with the beam on there were 2627 counts per second at the lowest beam intensity. Therefore, the observed effect has a negligible impact on the counts rate during measurements.

6 Conclusions

The beam profile at the CERF facility was measured with the Triple GEM detector at different beam intensities and was compared to the one obtained by the routinely used MWPC. Unlike the latter, the GEM detector showed no saturation at high beam intensity. In addition, it showed reasonable linearity when compared with the IC monitor, both with digital and current readout. The digital readout allows making a 2D online image of the beam and can be used for aligning the beam to the target. The beam intensity can also be monitored by means of the total current driven by the GEM foils.

Interruptions at high beam intensity observed on the FPGA will be eliminated in the future by unplugging it from the detector and placing it off the beam. Possible activation was observed after

2014 JINST 9 P06006

an intensity scan, which nonetheless produced a negligible number of counts as compared to the count rate with beam on.

The present study shows that the triple GEM detector holds the advantage of 2D online beam imaging with satisfactory counting capability, thus merging the characteristics of a MWPC and an IC. In addition, it allows having an experimental setup that rapidly centres the beam to the target and therefore optimises and speeds up the beam set-up time.

Acknowledgments

This research project has been supported by the Marie Curie Initial Training Network Fellowship of the European Community's Seventh Framework Program under Grant Agreement PITN-GA-4 2011-289198-ARDENT.

References

[1] F. Sauli, *GEM: A new concept for electron amplification in gas detectors*, *Nucl. Instrum. Meth.* **A 386** (1997) 531.

[2] A. Mitaroff and M. Silari, *The CERN-EU high-energy Reference Field (CERF) facility for dosimetry at commercial flight attitudes and in space*, *Radiat. Prot. Dosimetry* **102** (2002) 7.

[3] F.P. La Torre et al., *A new verification of the calibration factor of the CERF beam monitor*, CERN-RP-2013-083-REPORTS-TN (2013).

[4] A. Ferrari et al., *Monitoring reactions for the calibration of high-energy mixed hadron beams*, Submitted for publication in *Nucl. Instrum. Meth.* **A**.

[5] J. Spanggaard et al., *GEM detectors for the transverse profile measurement of low energy antiprotons and high energy hadrons*, CERN-ATS-2013-052, (2013).

[6] S. Bachmann et al., *Performance of GEM detectors in high intensity particle beams*, *Nucl. Instrum. Meth.* **A 470** (2001) 548.

[7] M. Alfonsi et al., *The triple-Gem detector for the M1R1 muon station at LHCb*, *IEEE Nucl. Sci. Simp. Conf. Rec.* **2** (2005) 811.

[8] M. Alfonsi et al., *High-rate particle triggering with triple-GEM detector*, *Nucl. Instrum. Meth.* **A 518** (2004) 106.

[9] W. Bonivento, P. Jarron, D. Moraes, W. Riegler and F. dos Santos, *Development of the CARIOCA front-end chip for the LHCb muon detector*, *Nucl. Instrum. Meth.* **A 491** (2002) 233.

[10] F. Murtas et al., *Applications in beam diagnostics with triple GEM detectors*, *Nucl. Instrum. Meth.* **A 617** (2010) 237.

[11] G. Corradi, F. Murtas and D. Tagnani, *A novel high-voltage system for a triple GEM detector*, *Nucl. Instrum. Meth.* **A 572** (2007) 96.

[12] G. Croci et al., *Measurements of γ-ray sensitivity of a GEM based detector using a coincidence technique*, 2013 *JINST* **8** P04006.

[13] A. Ferrari et al., *FLUKA: a multi-particle transport code*, CERN-2005-10 INFN/TC_05/11 SLAC-R-773 (2005).

[14] G. Battistoni et al., *The FLUKA code: Description and benchmarking*, Proceedings of the *Hadronic Shower Simulation Workshop 2006*, Fermilab, September 6–8 2006, M. Albrow and R. Raja eds., *AIP Conf. Proc.* **896** (2007) 31.

2014 JINST 9 P06006